This paper is submitted elsewhere and cannot be part of the conference proceedings

FEASIBILITY OF HIGH-TEMPERATURE ELECTROSTATIC PRECIPITATION FOR THE REMOVAL OF NANOPARTICLES: A CASE STUDY ON IRON OXIDE SEPARATION AT UP TO 800 °C

Patrick Bürger, M.Sc.*, Prof. Dr.-Ing. Ulrich Riebel
Lehrstuhl Mechanische Verfahrenstechnik
Brandenburgische Technische Universität Cottbus-Senftenberg
03013 Cottbus, Germany

ABSTRACT

The removal of nanoparticles from hot gas streams is a challenging task. On the other hand, there is a huge potential for heat recovery from waste gas incineration, glass furnaces, ceramic, metallurgical, pyrolytic and many other high temperature processes. Another relevant application is the separation of nanoparticles formed by condensation in thermal post-combustion processes, in order to achieve efficient heat recovery at high temperatures.

This case study evaluates the performance of a high-temperature electrostatic precipitator (HT-ESP) between 400 – 800 °C for both discharge polarities. The tube-type ESP with 150 mm diameter and 1500 mm length is operated isothermally. Two electrode designs are tested by separating flame-generated iron oxide nanoparticles from a flue gas atmosphere. The total number concentration in the raw gas is around $2 \cdot 10^{13}$ m^{-3} with a temperature-dependent mode diameter of 20 – 40 nm.

Between 400 – 600 °C very high separation efficiencies above 99.998 % (number-based) were found with just 1.5 s of residence time and negative polarity, using a wire discharge electrode requiring a moderate current density of 1.0 mA/m² up to 500 °C. In fact, the separation is more efficient than at room temperature which is explained by the occurrence of electronic charging with free electrons. This leads to exceptionally high particle charges compensating the reduced operating voltage. At 700 °C and 800 °C, separation efficiencies of 99.9 % and 99.5 % respectively (number-based) were obtained, using a rod discharge electrode for optimal use of thermionic emissions. The specific input of energy required for 99 % separation efficiency at any temperature is less than 150 J/m³, except for 800 °C with 250 J/m³.

These findings clearly prove that HT-ESPs are a feasible and highly performing alternative for nanoparticle removal from hot gases at up to 800 °C.

KEYWORDS

Electrostatic Precipitation, High-Temperature Gas Cleaning, Nanoparticles, Charging Mechanisms, Free Electrons, Thermionic Emission

1. Introduction

High-temperature (HT) gas cleaning above 400 °C is a complex endeavour. Therefore, it is often circumvented by cooling the gas before particle separation is attempted. The separation of nanoparticles at high temperatures is especially difficult because nanoparticle filter cakes on ceramic filters create a very high pressure loss and regeneration of the filters may be difficult due to sintering of the particles. However, a vast range of processes may benefit from efficient HT particle separation, such as processes involving gas turbines, heat exchangers, catalyst beds or the separation of products created under HT conditions.

Electrostatic precipitators (ESPs) are usually disregarded as an option above 400 °C due to steep current-voltage characteristics (CVCs) and reduced operating voltage. CVCs measured in particle free gases with negative polarity are especially affected and are often referred to for the temperature limit.

Between the 1960s and the 1980s high-temperature electrostatic precipitation was studied across the world due to the interest in high-temperature high-pressure combustion processes. The focus of these studies was on CVCs in particle-free gases, often exclusively using negative polarity and small dimensions of the collection electrode (Thomas and Wong 1958; Shale et al. 1963, 1964; Shale and Holden 1969; Bush et al. 1977). Some groups also investigated the separation efficiency by: (i) emulating a municipal waste incineration power plant at around 900 °C and 7.9 bar_{abs} resulting in 87 % separation efficiency with an unknown particle size and concentration using negative polarity (Brown and Walker 1971); (ii) demonstrating µm-scale fly ash removal in a temperature range of 743 – 916 °C at 6.4 bar_{abs} with separation efficiencies above 90 % with negative polarity (Rinard et al. 1987); (iii) or by testing fly ash removal on a semi-industrial scale with a plate-type ESP and different electrode designs at 650 – 770 °C and 5 – 16 bar_{abs} obtaining maximum separation efficiencies at 10 bar_{abs} of 93 % and 72 %, respectively (Weber et al. 1993).

Based on an increased number of publications, research on HT-ESPs regained traction during the last decade with a focus on particle separation from pyrolytic processes and flue gases generated by coal-based combustion processes (Villot et al. 2012; Xu et al. 2015; Ni et al. 2016; Zheng et al. 2017).

While HT-ESPs are a research topic since the 1960s, the charging mechanisms and the separation efficiency for nanoparticles have not been investigated in detail at higher temperatures. However, there are hints that the thermionic emission of electrons may have a strong influence on particle charging. This so called “electronic charging” was suspected in several studies on HT electrostatic precipitation but was never evaluated (Shale and Holden 1969; Weber et al. 1993). The reduced operating voltage at high temperatures will certainly affect the separation efficiency for large particles, but the increased range of free electrons will allow for highly effective electronic charging of nanoparticles. A previous study by the authors with technical N_2 revealed that an increased concentration of free electrons leads to astonishingly high separation efficiencies for sub-µm particles with operating voltages slightly above the onset voltage of the negative corona discharge (Bürger and Riebel 2020). This is due to the 3-fold higher particle charge obtainable with electronic charging compared to particle charging with ions at the same operating voltage (13 kV) in air, resulting in measured separation efficiencies of 99.997 % and 93.7 %, respectively.

The focus of this contribution will be on separation and energy efficiency of a HT-ESP operated with an iron oxide nanoparticle aerosol. Our results demonstrate that high separation efficiencies can be reached in the temperature range 400 – 800 °C even at atmospheric pressure. Further we provide an understanding about the contribution of free electrons to particle charging and separation success.

2. Experimental setup

The tube-type HT-ESP designed for this study can be operated isothermally between room temperature and 800 °C with both polarities. Figure 1 illustrates the design of the plant. The collection electrode has a diameter of 150 mm and a length of 1500 mm. Cone pieces are attached at both ends to prevent a convergence of field lines at the in-/outlet. Two discharge electrodes with different diameters are used, a classical wire electrode with 1 mm (E1) and an 8 mm rod electrode optimized for high temperatures (E2) to use the effect of thermionic emissions without a corona discharge. Both electrodes are centred by a ceramic MgO weight guided into a ceramic Al_2O_3 crucible at the bottom of the plant. Current losses at the HV-insertion are minimized by a special multilayer design consisting of two isolators, a feed-through electrode connecting the discharge electrode, and a tube electrode on the

same potential acting as a shield (for more details see: Bürger and Riebel 2022). The current is measured on the HV side at the feed-through electrode with a high resolution custom-build amperemeter.

The experiments are conducted in a flue gas atmosphere produced by an adjustable propane burner. An additional aerosol generator provides a flame generated iron oxide nanoparticle aerosol which is mixed with the flue gas in a thermally insulated burning chamber. The mass concentration is approx. 1.35 mg/m³ at a volumetric flow rate of 63.5 m³/h at operating temperature, corresponding to a gas velocity of 1 m/s in the ESP section. The flue gas enters the bottom of the ESP tangentially and is redirected by the cone piece to ensure homogeneous conditions regarding temperature, flow distribution and particle concentration.

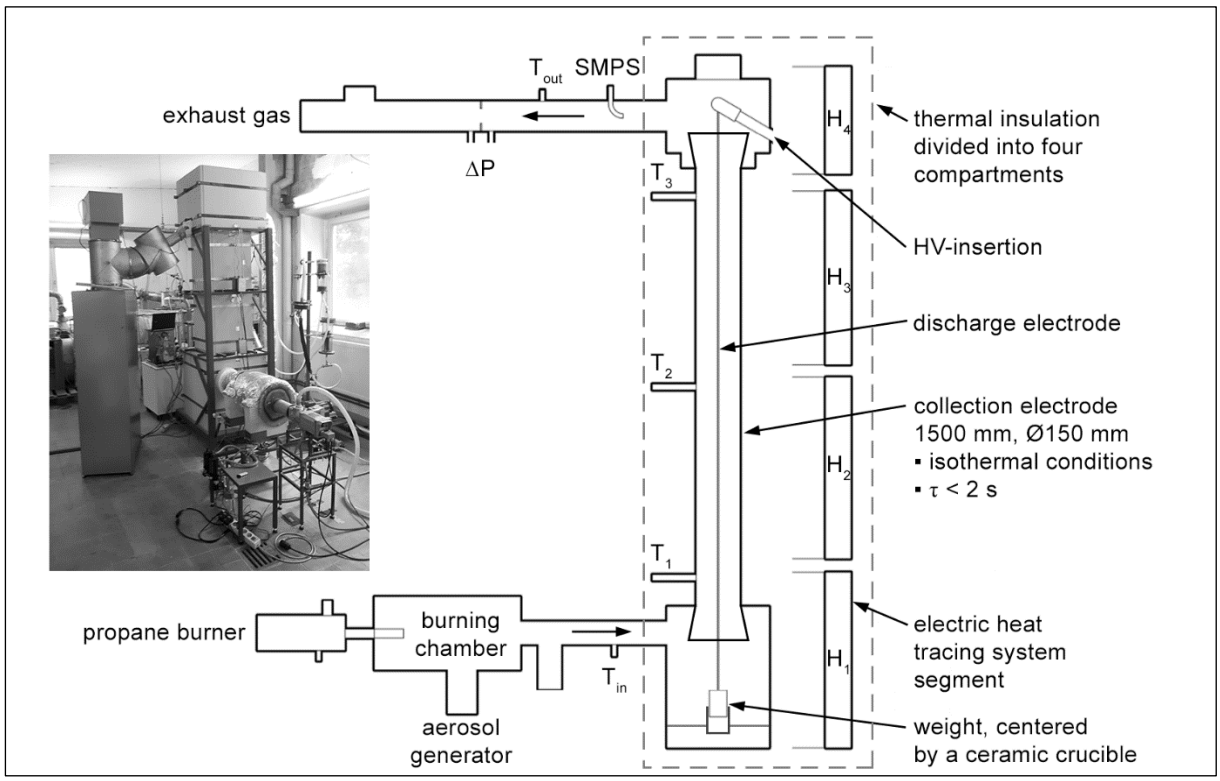

Figure 1 *Pilot-plant HT-ESP in wire-tube geometry, with a main collection tube diameter of 150 mm and 1500 mm length (w/o conical in-/outlet), a centred discharge electrode, and an operating temperature of up to 800 °C.*

Heat losses are compensated by an electrical heat tracing system with a multi-layered heat insulation. Several thermocouples are used to monitor and control temperature, especially in the ESP section. The exhaust gas section is equipped with an orifice plate for flow measurements, a sampling port for the dilution system and

subsequent SMPS measurements, and an associated thermocouple. Further downstream the exhaust gas is cooled down by mixing with ambient air and cleaned by a second ESP at moderate temperatures to protect the environment.

3. Results

3.1 Aerosol Characteristics

The characteristics of the iron oxide aerosol are temperature dependent because the coagulation coefficient and the Fuchs correction factor are a function of temperature. Therefore, the total number concentration (TNC) and the average diameter of the particles will change with operating temperature of the ESP. The particle size distributions (PSDs) of the raw gas for the investigated temperature range are presented in Figure 2. With increased temperature a shift towards smaller particle diameters is observed. At 700 °C and 800 °C the curves become steeper and narrower. At 400 °C the mode diameter is 40 nm with a TNC of $1.69 \cdot 10^{13}$ m^{-3} changing gradually to 21.7 nm and $2.64 \cdot 10^{13}$ m^{-3} at 800 °C.

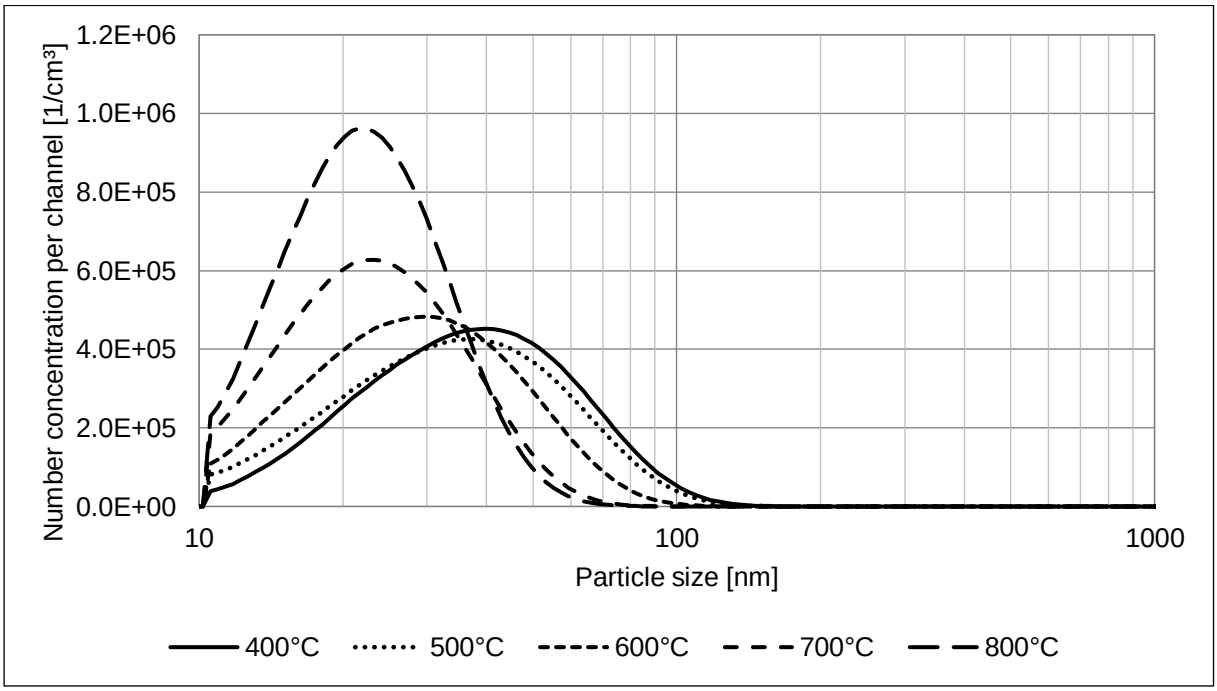

Figure 2 *Particle size distributions (PSD) of the iron oxide aerosol (raw gas) between 400 – 800 °C. The PSD becomes narrower and shifts towards smaller particles at higher temperatures due to effects on the coagulation process.*

While the residence time from the aerosol inlet to the sampling port does not change due to identical volume flow rates at all temperatures, the coagulation mechanisms

appear to be a function of temperature. This can be explained by a reduced coagulation efficiency of nanoparticles at higher temperatures (D'Alessio et al. 2005; Sirignano and D'Anna 2013).

3.2 Separation Efficiency and Specific Input of Energy

The separation efficiency and the energy efficiency in terms of specific input of energy (SIE) are very helpful metrics for the performance evaluation of HT-ESPs. Experiments were conducted between 400 – 800 °C with the wire electrode (E1). The HT-optimized electrode (E2) was investigated from 600 to 800 °C afterwards. The pilot plant is operated with a gas velocity of 1 m/s commonly used in industrial ESPs leading to a residence time of 1.5 s. The short residence time in the ESP section allows to distinguish clearly between different operation points. At each temperature the performance of E1 was assessed at 5 kV (below onset voltage), for three current densities covering typical industrial settings (0.25 mA/m², 0.5 mA/m², 1.0 mA/m²) and at 3 mA/m² for heavy duty operation. E2 was tested at predetermined operating voltages starting at 5 kV with increments of 2.5 kV, when possible. Due to sparking or damage prevention precautions not all predefined settings were completed at all temperatures. Figure 3 summarizes the best results in terms of overall particle penetration for both electrodes and polarities which usually is the highest predefined setting reached. All settings will be shown in the evaluation of the energy efficiency.

Between 400 – 600 °C the wire electrode E1 shows very high separation efficiencies, especially with negative polarity which clearly indicates electronic charging by free electrons. At each temperature investigated in this range 99.999 % of the particles can be removed in just 1.5 seconds of residence time (number-based). While negative polarity sustains its performance at the highest current density up to 600 °C, positve polarity shows an increasing particle penetration with temperature. At 400 °C and 500 °C negative polarity reaches 99.998 % separation efficiency with an industrially relevant current density of 1.0 mA/m² (not shown in Fig. 3).

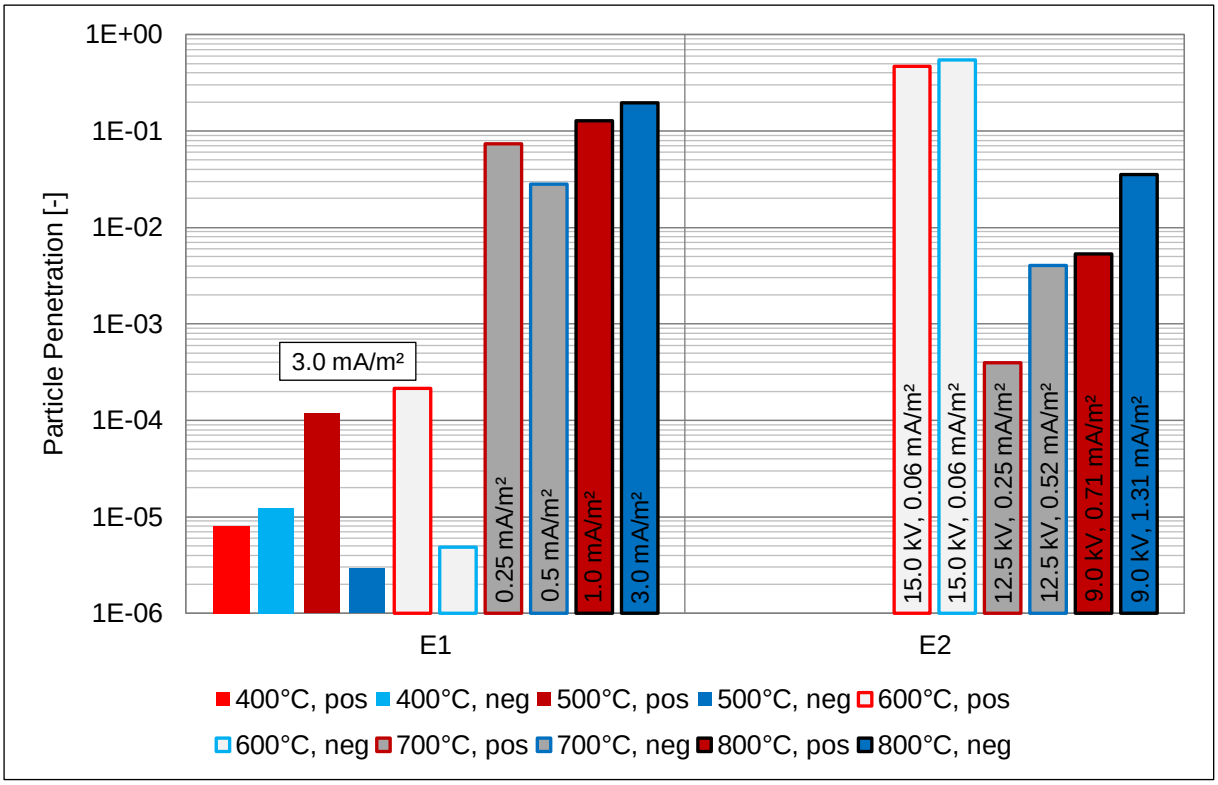

Figure 3 *Lowest overall particle penetration, measured with both polarities for a wire electrode (E1) between 400 – 800 °C (current density based on collection electrode surface area), and for a HT-optimized electrode (E2) between 600 – 800 °C.*

At 700 °C and 800 °C the performance with E1 drops significantly, with 93 % and 87 % for positive polarity and 97 % and 80 % for negative polarity, respectively. At these temperatures several factors prevent a better separation efficiency with the wire electrode. For both polarities, the operating voltage decreases strongly for a given current density, especially for negative polarity, which has an adverse effect on particle migration in the electric field. For positive polarity, the thermionic emission of free electrons from the collection electrode causes bipolar charging which results in a lower positive particle charge or even a polarity change. For negative polarity, an increasing thermionic emission of electrons from the particle surface limits the maximum particle charge. These explanations are based on the measurements of the particle mobility distribution without prior aerosol neutralisation and calculations of the particle charge from the experimental data (not shown in this contribution).

While this performance may suffice as a first pre-treatment to protect subsequent equipment from dust layers at 700 °C and above, it is not satisfactory as a stand-alone solution even with increased residence time. Therefore, the HT-optimized discharge electrode (E2) was designed to improve performance by utilizing

thermionic emission of electrons. The results at 600 °C show that thermionic emission does not improve separation efficiency yet, even at higher voltages compared to E1 at 3 mA/m² (12 kV vs. 15 kV). Here, the particle separation is based on the bipolar charge of the aerosol obtained in the flame during generation. The precharged particles travel in the field towards the electrodes and are collected upon arival. However, at 700 °C positive polarity achieves a separation efficiency of 99.96 % (neg. polarity: 99.6 %), which may be even higher if one had deviated from the predifined voltage steps (15 kV was not possible due to sparking). Performance decreases slightly at 800 °C due to reduced operating voltages (max. 9 kV possible), but positive polarity maintains a respectable separation efficiency of 99.5 % while negative polarity drops down to 96.5 %. A design change of the HV insertion should allow for even higher voltages and subsequent higher separation efficiencies, since it was optimized for accurate current measurements even below onset voltage. In an industrial application operating voltages close to spark-over in the ESP section should be obtained easily due to larger clearances at the HV insertion and simplified cooling approaches. Nevertheless, these results prove that ESPs can be operated successfully at temperatures of up to 800 °C, despite of reduced operating voltages.

At high temperatures the operating voltage decreases significantly for a given current density while a constant operating voltage yields a higher current density. Assessing energy efficiency of ESPs at high temperatures gives interesting insights on the influence of temperature. The specific input of energy (SIE) relates the electrical power to the volumetric flow rate in the ESP (giving J/m³) which is comparable to the pressure drop of a filtration media since the Δp in an ESP is neglectable (see Eq. 1).

$$\Delta p \mathrel{\widehat{=}} SIE = \frac{U \cdot I}{\dot{V}} \tag{1}$$

In Figure 4 the particle penetration is plotted against the SIE on a log-log scale for both polarities. In order to demonstrate the efficiency of electronic charging by free electrons at high temperature, results obtained previously in technical nitrogen are included in the figure to serve as a reference (Bürger and Riebel 2020). Highly efficient electronic charging occurs with negative polarity in technical nitrogen due to an increased range of electrons caused by reduced ion formation with oxygen (black

line with × markers). Positive polarity on the other hand does not deviate from typical operation in air (black line w/o markers).

Figure 4a shows the results for E1 (○ markers) and E2 (□ markers) for positive polarity. Up to 600 °C the results are grouped closely with an increase in SIE at higher temperatures. Using 99.9 % separation efficiency as an arbitrary threshold, the SIE doubles for E1 at 600 °C compared to 350 J/m³ at 400 °C. At 700 °C and above the separation efficiency is barely improved by increasing the SIE which points towards a disturbance of particle charging and separation. While E2 does not give good results at 600 °C, it is capable of very efficient particle separation at 700 °C. At 800 °C the separation efficiency of E2 (99.5 % at 9 kV) is comparable to E1 at 600 °C with a SIE of 250 J/m³.

Figure 4b presents the results for negative polarity where E1 behaves mostly comparable. The ESP operates very efficiently between 400 – 500 °C and remains on low SIE values even at separation efficiencies of 99.999 %. This changes at 600 °C for lower SIE values since the particle penetration increases visibly. A higher SIE leads to comparable results as at lower temperatures. At 700 °C and above the steep CVCs with E1 strongly reduce the operating voltage at a given current which explains the low performance in terms of SIE and separation efficiency. E2 ensures higher separation efficiencies than E1 at 700 °C and 800 °C but is less efficient with negative polarity. This is caused by higher currents at a given voltage which is not compensated by better charging with increased numbers of free electrons.

Compared to the reference values obtained at room temperature in technical nitrogen by Bürger and Riebel (2020), electrostatic precipitation at higher temperature usually requires less energy for a certain separation efficiency, at least for the removal of nanoparticles. Despite the short residence time, 99 % separation efficiency can be obtained with less than 250 J/m³ between 400 – 800 °C. In most cases less than 150 J/m³ are required (based on best electrode/polarity combination).

These values represent upper limits since considerable leak currents were detected at 600 °C and above, leaking via the ceramic weight. For comparative reasons the MgO weight (see Fig. 1) was attached to both electrode designs during the separation efficiency experiments. Afterwards, E2 was tested at 700 °C without the

weight by obtaining CVCs and conducting separation efficiency experiments with both polarities. Considerable leak currents via the ceramic weight and crucible were measured which have a negative impact on the energy efficiency of the HT-ESP.

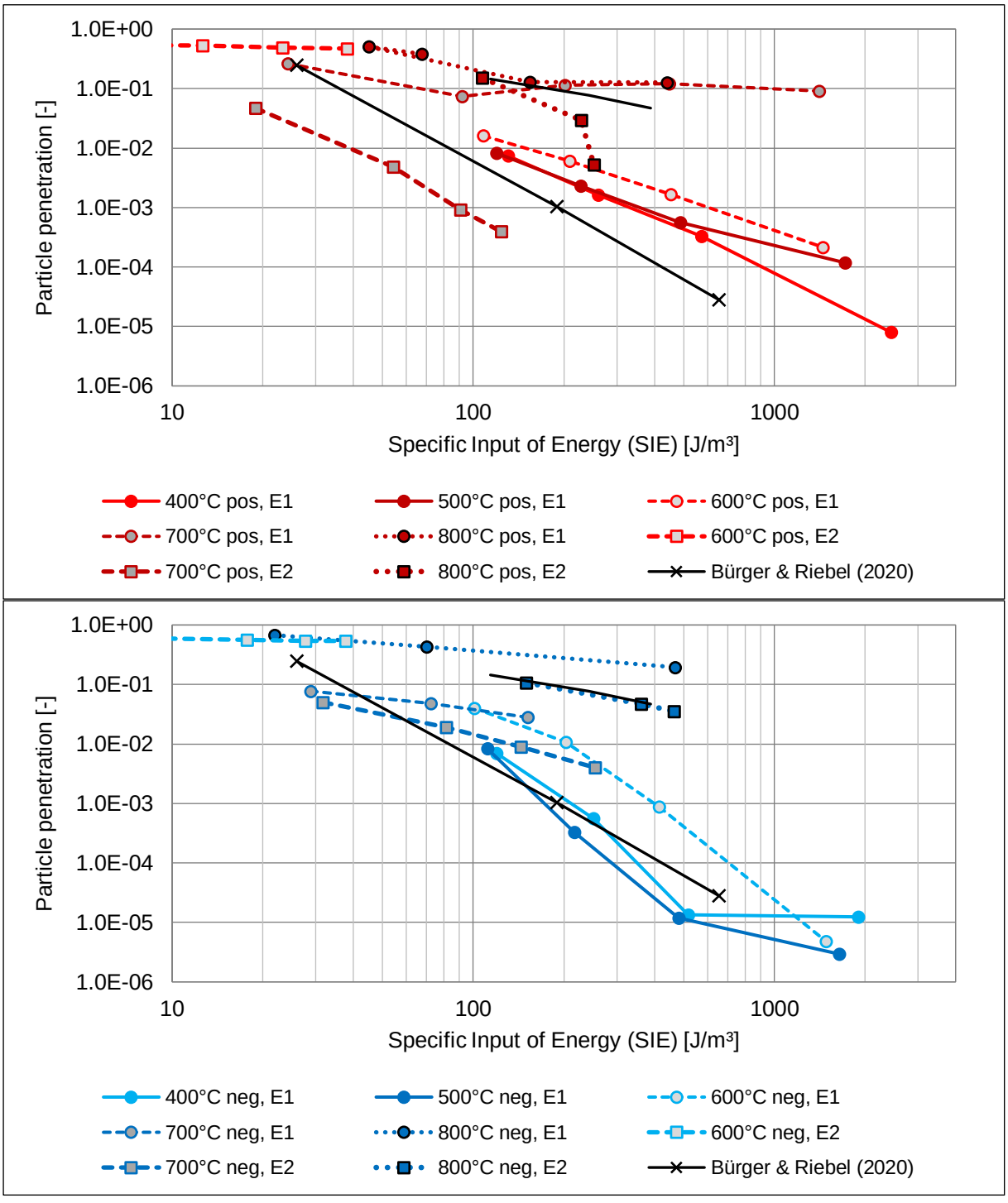

Figure 4 *Particle penetration as a function of SIE at operating conditions. The black line with × markers represents results in tech. N_2 with neg. polarity (highly efficient electronic charging) from Bürger & Riebel (2020). The black line w/o markers shows results in tech. N_2 with pos. polarity, same authors (comparable to pos. polarity in air).* ***(a)*** *Results for positive polarity (above).* ***(b)*** *Results for negative polarity (below).*

For E1 this plays a minor role since the leak currents contribute only around 20 % at 1 mA/m² and 700 °C due to the high currents from the corona discharge. However, for E2 at 700 °C and 10 kV a comparable leak current results in a share of 90 % from the total current. This issue can be solved easily in an industrial-size HT-ESP. The experiment without the weight showed that only 13.7 J/m³ are required for a separation efficiency of 99.5 % which is only 25 % of the SIE compared to the experiment with the weight suffering from leak currents.

4. Discussion

The operating temperature influences ESP operation at a constant pressure in multiple ways via the gas density, the mean free path length (ions, electrons) and the behaviour of the ionization processes. An increase in temperature at fixed pressure will cause:

- a decrease in gas density and an increase in mean free path length,
- a reduction of the onset and spark-over voltage,
- an increase of current at a given voltage,
- an increase of ion mobility by limiting cluster ion formation,
- an increase of free electron reach raising the apparent ion mobility,
- and an increase of thermionic electron emissions at very high temperatures.

While these dependencies lead to steep CVCs and a reduced operating voltage range at high temperatures, especially with negative polarity, they also offer interesting possibilities for the charging and separation of nanoparticles. Typically, particle charging is driven by gas ions which transfer their charge to a particle upon contact. The collision between a gas ion and a particle can be described by the mechanisms of diffusion charging and field charging. Both occur simultaneously but field charging becomes more relevant at larger particle sizes (> 500 nm). With increasing temperature, the maximum available field strength diminishes due to the reduced operating voltage and the field charging mechanism loses performance. Diffusion charging by gas ions on the other hand is enhanced slightly by higher temperatures due to the increased thermal velocity of the ions, increased diffusivity, and reduced cluster ion formation. Additionally, with increasing temperature the attachment process of electrons onto gas molecules becomes less efficient which leads to considerable concentrations of free electrons in the drift zone. Free electrons

can attach to particles via the mechanism of electronic diffusion charging and can lead to very high charges on nanoparticles due to their extreme thermal velocity. The significantly increased particle charge q can compensate for the lower electric field E at higher temperatures, as the electric field is also the driving force for particle migration. Furthermore, the higher mean free path length at a fixed pressure will increase the electric mobility of particles, which is described by the Cunningham correction Cu. Equation 2 shows the dependency of the migration velocity $v_{mig.}$ from the electric mobility Z_{el} and the electric field E, where η is the gas viscosity and d_p the particle diameter.

$$v_{mig.} = Z_{el} \cdot E = \frac{q \cdot Cu}{3 \cdot \pi \cdot \eta \cdot d_p} \cdot E \tag{2}$$

Comparing the results between 400 – 600 °C from both polarities (see Fig. 3) the strong effect of electronic charging on separation efficiency is clearly visible, similar to our experiments in technical nitrogen (Bürger and Riebel 2020).

At temperatures of 700 °C and above thermionic emission of electrons becomes relevant for ESP operation. The separation efficiency of experiments with positive polarity and E1 is dropping due to bipolar charging effects caused by the electrons emitted from the collection electrode. Experiments with negative polarity and E1 cannot utilize the increased number of electrons emitted from the wire due to strongly reduced electric fields at a given current density. The HT-optimized E2 on the other hand uses thermionic emissions to an advantage with both polarities by staying below the onset voltage. This means that even with positive polarity no positive gas ions are generated and the particle charge will be negative for both polarities. Surprisingly, positive polarity outperforms negative polarity with E2 at a given voltage which may be connected to either: (i) the larger surface area of the collection electrode (despite lower currents measured for pos. polarity), (ii) a more uniform distribution of electrons or (iii) a dependency of particle charging on the kinetic energy of electrons. In any case, more research on electronic charging is required to understand the reasons behind this. It has to be mentioned that in this scenario the particles are deposited on the discharge electrode when applying positive polarity due to the negative charges on the particles. This must be considered in the design of the dedusting mechanism if the ESP is operated with positive polarity.

On a side note, this HT-ESP setup may slightly benefit from an increasingly laminar flow at 1 m/s gas velocity and higher temperatures facilitating particle migration towards the collection electrode. Typically, the electrohydrodynamic wind counters such an effect but in symmetric geometries and uniform discharges (e.g., positive polarity) an influence on separation efficiency by a laminar flow can be observed.

5. Conclusion

In this study the separation of iron oxide nanoparticles from flue gas was demonstrated with a tube-type ESP in a temperature range between 400 – 800 °C. Two discharge electrode designs were tested in a pilot plant setup with a 1500 mm long and 150 mm wide collection electrode. The gas velocity was kept constant at 1 m/s for every temperature resulting in a very short residence time of 1.5 s. However, a number-based separation efficiency above 99.9 % was achieved at temperatures up to 700 °C while at 800 °C the maximum was 99.5 %. Remarkable separation efficiencies are obtainable with a wire electrode (E1) between 400 – 600 °C with both polarities (above 99.98 %). Even higher separation efficiencies above 99.998 % are obtained with negative polarity. This can be explained by highly effective charging with free electrons. Electronic charging allows for a much higher particle charge compensating the reduced operating voltage. At 700 °C and above the design of the discharge electrode must be adapted to utilize thermionic emissions of electrons in order to achieve good separation efficiency. The optimized electrode (E2) reaches higher operating voltages while limiting the current to moderate levels.

Surprisingly, particle charging and removal are more energy efficient compared to ESP operation near ambient temperature given the fact, that the gas is provided hot. High separation efficiencies can be reached for nanoparticles at up to 800 °C even with short residence times. Increasing the residence time from 1.5 to 3 s results in even better performance which will be sufficient for any application in the temperature range investigated. Therefore, clear evidence is given that HT-ESPs are a feasible and energy efficient concept for the removal of nanoparticles.

Abbreviations

CVC: current-voltage characteristics; E1: electrode 1; E2: electrode 2; ESP: electrostatic precipitator; HT: high-temperature; HV: high voltage; PSD: particle size distribution; SIE: specific input of energy; SMPS: scanning mobility particle sizer; TNC: total number concentration

References

Brown R.F., Walker A.B. (**1971**) Feasibility Demonstration of Electrostatic Precipitation at 1700°F. *Journal of the Air Pollution Control Association*, 21, pp. 617–620. https://doi.org/10.1080/00022470.1971.10469576

Bürger P., Riebel U. (**2020**) Electrostatic charging and precipitation of nanoparticles in technical nitrogen: Highly efficient diffusion charging by hot free electrons. *Journal of Aerosol Science*, 141. 105495. https://doi.org/10.1016/j.jaerosci.2019.105495

Bürger P., Riebel U. (**2022**) High temperature coronas in air and flue gas from LPG combustion: Current-voltage characteristics, ion mobilities and free electrons. *Journal of Electrostatics*, 115, 103676. https://doi.org/10.1016/j.elstat.2022.103676

Bush J.R., Feldman P.L., Robinson M. (**1977**) Development of a high-temperature/high-pressure electrostatic precipitator: Final report August 1975--August 1977, United States. https://nepis.epa.gov/Exe/ZyPURL.cgi?Dockey=9101EDTR.txt. Accessed 31 March 2020

D'Alessio A., Barone A.C., Cau R., D'Anna A., Minutolo P. (**2005**) Surface deposition and coagulation efficiency of combustion generated nanoparticles in the size range from 1 to 10nm. *Proceedings of the Combustion Institute*, 30, pp. 2595–2603. https://doi.org/10.1016/j.proci.2004.08.267

Ni M., Yang G., Wang S., Wang X., Xiao G., Zheng C., Gao X., Luo Z., Cen K. (**2016**) Experimental investigation on the characteristics of ash layers in a high-temperature wire–cylinder electrostatic precipitator. *Separation and Purification Technology*, 159, pp. 135–146. https://doi.org/10.1016/j.seppur.2016.01.011

Rinard G., Rugg D.E., Yamamoto T. (**1987**) High-Temperature High-Pressure Electrostatic Precipitator Electrical Characterization and Collection Efficiency. *IEEE Transactions on Industry Applications*, IA-23, pp. 114–119. https://doi.org/10.1109/TIA.1987.4504875

Shale C.C., Bowie W.S., Holden J.H., Strimbeck G.R. (**1963**) Feasibility of electrical precipitation at high temperatures and pressures: Report of Investigations 6325, Washington

Shale C.C., Bowie W.S., Holden J.H., Strimbeck G.R. (**1964**) Characteristics of positive corona for electrical precipitation at high temperatures and pressures: Report of Investigations 6397, Washington

Shale C.C., Holden J.H. (**1969**) The Role of Wire Size in Negative Electrical Discharge at High Temperature. *IEEE Transactions on Industry and General Applications*, IGA-5, pp. 34–39. https://doi.org/10.1109/TIGA.1969.4180985

Sirignano M., D'Anna A. (**2013**) Coagulation of combustion generated nanoparticles in low and intermediate temperature regimes: An experimental study. *Proceedings of the Combustion Institute*, 34, pp. 1877–1884. https://doi.org/10.1016/j.proci.2012.06.119

Thomas J.B., Wong E. (**1958**) Experimental Study of DC Corona at High Temperatures and Pressures. *Journal of Applied Physics*, 29, pp. 1226–1230. https://doi.org/10.1063/1.1723407

Villot A., Gonthier Y.F.J., Gonze E., Bernis A., Ravel S., Grateau M., Guillaudeau J. (**2012**) Separation of particles from syngas at high-temperatures with an electrostatic precipitator. *Separation and Purification Technology*, 92, pp. 181–190. https://doi.org/10.1016/j.seppur.2011.04.028

Weber E., Wiggers H., Morgenstern U. (**1993**) Erprobung eines Plattenelektrofilters fuer die Erprobung eines Plattenelektrofilters für die Hochtemperatur-Hochdruck-Entstaubung unter Berücksichtigung spezieller Effekte. *Luft und Kältetechnik*, 4, pp. 165–168

Xu X., Gao X., Yan P., Zhu W., Zheng C., Wang Y., Luo Z., Cen K. (**2015**) Particle migration and collection in a high-temperature electrostatic precipitator. *Separation and Purification Technology*, 143, pp. 184–191. https://doi.org/10.1016/j.seppur.2015.01.016

Zheng C., Shen Z., Chang Q., Su Q., Zhu X., Gao X. (**2017**) Experimental Study on Electrostatic Precipitation of Low-Resistivity High-Carbon Fly Ash at High Temperature. *Energy & Fuels*, 31, pp. 6266–6273. https://doi.org/10.1021/acs.energyfuels.7b00107